Generation, Characterization, and Reactivity of the Transition Metal−*o*-Benzyne Analog of Pyrazine (Fe^+−2,3-Didehydropyrazine) in the Gas Phase: An Experimental and Theoretical Study

Huiping Chen, Denley B. Jacobson,* and Ben S. Freiser†

H. C. Brown Laboratory of Chemistry, Purdue University, West Lafayette, Indiana 47907

Received November 13, 1998

Fe^+−2,3-didehydropyrazine (**2**) has been generated and its reactivity with simple olefins and alkynes studied by using Fourier transform ion cyclotron resonance (FTICR) mass spectrometry. **2**, which is prepared by dehalogenation of chloropyrazine by Fe^+, undergoes a simple adduct formation (no ligand coupling) with ethene and ethene-d_4. Ethyne also yields adduct formation; however, ligand coupling has clearly occurred in this reaction. Interestingly, reactions with propene and isobutene yield the same products with similar product distributions. Again, ligand coupling is involved and a metal-centered mechanism featuring activation of the allylic carbon−hydrogen bonds is proposed. Propyne, allene, 1-butene, and *cis*-2-butene yield a variety of products with **2**. However, **2** yields exclusive dehydrogenation with 1,3-butadiene to generate $FeC_8H_6N_2^+$. CID results suggest that this $FeC_8H_6N_2^+$ ion consists of quinoxaline bound to Fe^+. Ligand displacement reactions yield a bond dissociation energy of 47 ± 5 kcal/mol for $D°(Fe^+-\text{quinoxaline})$. $FeC_4H_2N_2^+$ ion (**2**) has also been investigated theoretically. Density functional calculations predicted that the ground state of 2,3-didehydropyrazine is the triplet state, with the singlet state being 9.9 kcal/mol higher than the triplet state. **2** has C_{2v} symmetry with the metal center coplanar with the 2,3-didehydropyrazine ring. **2** has a sextet ground state with doublet and quartet states 4.9 and 6.8 kcal/mol higher, respectively. The bond dissociation energy $D°(Fe^+-C_4H_2N_2)$ for the sextet ground state is computed to be 87 ± 10 kcal/mol.

Introduction

o-Benzyne (C_6H_4) is intrinsically unstable and highly reactive due to the high degree of strain associated with the C−C triple bond.[1] However, *o*-benzyne can be stabilized by complexation of the C−C triple bond with a transition-metal center.[2] In fact, *o*-benzyne complexes of several transition metals have been isolated and crystallized.[3−6] Metal−*o*-benzyne ions, $MC_6H_4^+$ (M = Fe, Co, Sc, Fe_2) were generated in the gas phase by elimination of hydrogen halides from halobenzenes and their reactivities toward simple hydrocarbons extensively studied.[2,7−16] These studies have been extended to include Fe^+−naphthyne, which was generated via a similar reaction of Fe^+ with 1-fluoronaphthalene.[17] The realm of benzenoid aromatic compounds is not limited to benzene, naphthalene, and similar homocyclic compounds but also includes, among others, five- and six-membered heterocyclic compounds (tetrahydrofuran, pyridine, etc.). The benzyne analogues of these compounds are generally called *dehydroaromatics* or *hetarynes*.[1]

In comparison to *o*-benzyne, the hetarynes are considerably more complex and, potentially, more interesting. A number of hetarynes have been studied in the past few decades.[18,19] Hetarynes are believed to be important intermediates in nucleophilic substitutions on heterocyclic aryl halides.[18−24] Principal attention has focused on the 1,2-didehydroaromatics derived from

* To whom correspondence should be addressed. Present address: Department of Chemistry, Purdue University, West Lafayette, IN 47907. Permanent address: Department of Chemistry, North Dakota State University, Fargo, ND 58104.
† Deceased on December 31, 1997.

(1) Hoffman, R. W. *Dehydrobenzene and Cycloalkynes*; Academic Press: New York, 1967.
(2) Dietz, T. G.; Chatellier, D. S.; Ridge, D. S. *J. Am. Chem. Soc.* **1978**, *100*, 4905.
(3) McLain, S. J.; Schrock, R. R.; Sharp, P. R.; Churchill, M. R.; Youngs, W. J. *J. Am. Chem. Soc.* **1979**, *101*, 263.
(4) Churchill, M. R.; Youngs, W. J. *Inorg. Chem.* **1979**, *18*, 1697.
(5) Sarry, B.; Schaffernicht, R. *Z. Naturforsch., B: Anorg. Chem., Org. Chem.* **1981**, *36B*, 1238.
(6) Bennett, M. A.; Hambley, T. W.; Roberts, N. K.; Robertson, B. B.; *Organometallics* **1985**, *4*, 1992.
(7) Bjarnason, A.; Taylor, J. W. *Organometallics* **1989**, *8*, 2020.
(8) Bjarnason, A. *Organometallics* **1991**, *10*, 1244.
(9) Huang, Y.; Freiser, B. S. *J. Am. Chem. Soc.* **1989**, *111*, 2387.
(10) Huang, Y.; Freiser, B. S. *Inorg. Chem.* **1990**, *29*, 1102.
(11) Huang, Y.; Freiser, B. S. *J. Am. Chem. Soc.* **1990**, *112*, 1682.
(12) Huang, Y.; Freiser, B. S. *Inorg. Chem.* **1991**, *30*, 3822.
(13) Wittneben, D.; Grüzmacher, H. F.; Butenschön, H.; Wey, H. G. *Organometallics* **1992**, *11*, 3111.
(14) Garcia, E.; Huang, Y.; Freiser, B. S. *Inorg. Chem.* **1993**, *32*, 3595.
(15) Kan, S. Z.; Byun, Y. G.; Lee, S. A.; Freiser, B. S. *J. Mass Spectrom.* **1995**, *30*, 194.
(16) Kan, S. Z.; Byun, Y. G.; Freiser, B. S. *J. Am. Chem. Soc.* **1995**, *117*, 1177.
(17) Kan, S. Z.; Xu, C. Y.; Chen, Q.; Freiser, B. S. *J. Mass Spectrom.* **1997**, *32*, 1310.
(18) Kauffmann, Th. *Angew. Chem., Int. Ed. Engl.* **1965**, *4*(7), 543.
(19) ven Hertog, H. J.; van der Plas; H. C. *Advances in Heterocyclic Chemistry*; Academic Press: New York, 1965; Vol. 4, p 121.
(20) Adam, W.; Grimison, A.; Hoffmann, R. *J. Am. Chem. Soc.* **1969**, *91*, 2590.

10.1021/om980924j CCC: $18.00
Publication on Web 04/26/1999

nitrogen heterocyclics such as pyridine, quinoline, isoquinoline, and the various diazines.[1,18−24] Didehydropyrazine, on the other hand, has received relatively little attention. As the heterocyclic analogue of *o*-benzyne (1,2-dehydrobenzene), 2,3-didehydropyrazine (**1**) is the only isomer that can be drawn for the didehydropyrazine due to the symmetrical presence of the two nitrogen atoms.

1

2,3-Didehydropyrazine is believed to be an intermediate in the pyrolysis of pyrazine-2,3-dicarboxylic anhydride.[25] A strong peak at *m*/*z* ratio 78, corresponding to the didehydropyrazine ion, is observed in the mass spectrum of the anhydride. There have been a number of theoretical papers dealing with 2,3-didehydropyrazine; however, they were restricted to date to semiempirical calculations.[20,26−30] In contrast to *o*-benzyne, 2,3-didehydropyrazine has not been directly observed. In principle, coordination to a transition metal could yield stable 2,3-didehydropyrazine complexes, as found for metal−*o*-benzynes.[3−6]

As an extension of our earlier interests in the M^+−benzyne system, we are interested in exploring the generation and characterization of the reactivity of M^+−2,3-didehydropyrazine complexes. In this paper, Fe^+−2,3-didehydropyrazine (**2**) has been generated by elimi-

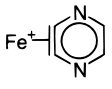

2

nation of HCl from chloropyrazine and its gas-phase reactions with selected small alkenes and alkynes have been studied by Fourier transform ion cyclotron resonance (FTICR) mass spectrometry. Reactions of *o*-benzyne with alkenes generally fall into one of three categories: (i) cycloaddition reactions with monoenes, (ii) ene reactions, and (iii) Diels−Alder reactions.[31] Our previous study on the reactions of Fe^+−benzyne with small alkenes showed active participation of the Fe^+ center in the reactions as well as direct ligand coupling.[11] The presence of the nitrogen atoms in the 2,3-didehydropyrazine ligand should affect the reactivity of the iron complex. Therefore, the reactions between Fe^+−2,3-didehydropyrazine with the same series of hydrocarbons as used for Fe^+−*o*-benzyne have been examined to further our understanding of factors important in controlling chemistry.

The geometries and thermodynamics of both 2,3-didehydropyrazine (**1**) and Fe^+−2,3-didehydropyrazine (**2**) were probed by density functional theory (DFT) methods. DFT methods are attractive because they include the effects of electron correlation. There is growing evidence that DFT is capable of providing a unified theoretical framework for the study of transition-metal systems.[32−37] Here we examine both the ground state and excited states of 2,3-didehydropyrazine and Fe^+−2,3-didehydropyrazine.

Experimental and Computational Section

All experiments were performed by using a Nicolet (now Finnigan FT/MS, Madison, WI) prototype FTMS-1000 Fourier transform ion cyclotron resonance (FTICR) mass spectrometer, equipped with a 5.2 cm cubic trapping cell situated between the poles of a Walker Scientific 15-in. electromagnet maintained at 1 T.[38] The cell has two 80% transmittance stainless steel mesh transmitter plates, and one of them holds various metal targets. Laser desorption ionization was used to generate Fe^+ by focusing the fundamental beam (1064 nm) of a Quanta-Ray Nd:YAG laser on a high-purity iron foil attached to the rear transmitter plate.[39] Chemicals were obtained commercially and used as supplied, except for multiple freeze−pump−thaw cycles to remove noncondensable gases. A static pressure of 1×10^{-5} Torr of argon was used throughout these experiments and serves both as the facilitator of ion thermalization prior to reaction and as the target for collision-induced dissociation (CID).[40]

Details for CID in conjunction with FTICR have been described elsewhere.[38] CID breakdown curves were obtained by varying the kinetic energy of the ions (typically between 1 and 30 eV) by adjusting either the duration of the CID electric field (typically between 100 and 600 μs) or the magnitude of the electric field pulse. The maximum translational energy acquired by an irradiated ion (in excess of thermal energy) in the laboratory frame was calculated by using the equation

$$E_{tr}(\max) = \frac{E^2 q^2 t^2}{16 M_{ion}}$$

where E is the electric field amplitude, t is the duration of the applied electric field, q is the ion charge, and M_{ion} is the mass of the irradiated ion.[41,42] CID fragment ion intensities are plotted as a fraction of the total ion intensities at each kinetic energy for CID breakdown curves.

(21) Gilchrist, T. L.; Gymer, G. E.; Rees, C. W. *J. Chem. Soc., Chem. Commun.* **1973**, 819.
(22) Gilchrist, T. L.; Gymer, G. E.; Rees, C. W. *J. Chem. Soc., Perkin Trans. 1* **1975**, 1747.
(23) Klinge, D. E.; van der Plas, H. C. *Recl. Trav. Chim. Pays-Bas* **1976**, *95*, 34.
(24) De Sio, F.; Chimichi, S.; Nesi, R.; Cecchi, L. *Heterocycles* **1982**, *19*(8), 1427.
(25) Brown, R. F. C.; Crow, W. D.; Solly, R. K. *Chem. Ind. (London)* **1966**, 343.
(26) Yonezawa, T.; Konishi, H.; Kato, H. *Bull. Chem. Soc. Jpn.* **1969**, *42*, 933.
(27) Jones, H. L.; Beveridge, D. L. *Tetrahedron Lett.* **1964**, 1577.
(28) Dewar, M. J. S.; Ford, G. P. *J. Chem. Soc., Chem. Commun.* **1977**, 539.
(29) Dewar, M. J. S.; Kuhn, D. R. *J. Am. Chem. Soc.* **1984**, *106*, 5256.
(30) Radom, L.; Nobes, R. H.; Underwood, D. J.; Li, W. K. *Pure Appl. Chem.* **1986**, *58*(1), 75.
(31) Kato, M.; Okamoto, Y.; Chidamoto, T.; Miwa, T. *Bull. Chem. Soc. Jpn.* **1978**, *51*, 1163.
(32) Holthausen, M. C.; Fiedler, A.; Schwarz, H.; Koch, W. *J. Phys. Chem.* **1996**, *100*, 6236.
(33) Labanowski, J. K.; Andzelm, J. W. *Density Functional Methods in Chemistry*; Springer-Verlag: New York, 1991.
(34) Siegbahn, P. E. M. *Adv. Chem. Phys.* **1996**, *93*, 333.
(35) Ricca, A.; Bauschlicher, C. W., Jr. *Chem. Phys. Lett.* **1995**, *245*, 150.
(36) Ricca, A.; Bauschlicher, C. W., Jr. *Theor. Chim. Acta* **1995**, *92*, 123.
(37) Ricca, A.; Bauschlicher, C. W., Jr. *J. Phys. Chem.* **1995**, *99*, 5922.
(38) Freiser, B. S. *Talanta* **1985**, *32*, 697.
(39) Cody, R. B.; Burnier, R. C.; Reents, W. D., Jr.; Carlin, T. J.; McCrery, D. A.; Lengel, R. K.; Freiser, B. S. *Int. J. Mass Spectrom. Ion Processes* **1980**, *33*, 37.
(40) Burnier, R. C.; Cody, R. B.; Freiser, B. S. *J. Am. Chem. Soc.* **1982**, *104*, 7436.
(41) Grosshans, P. B.; Marshall, A. G. *Anal. Chem.* **1991**, *63*, 2057.
(42) Freiser, B. S. In *Techniques for the Study of Ion Molecule Reactions*; Farrar, J. M., Saunders: W. H., Jr., Eds.; Wiley: New York, 1988; p 61.

In addition to conventional FTICR-CID, CID by using sustained "off-resonance" irradiation (SORI)[43] for ion activation was also employed to determine the lowest energy fragmentation pathways. For SORI-CID, ions are irradiated "off-resonance" for 500 ms. The *maximum* ion kinetic energy is calculated by using the equation

$$E_{tr}(\max) = \frac{E^2 q^2}{2M_{\text{ion}}(\omega_1 - \omega_c)^2}$$

where ω_1 (rad s^{-1}) is the excitation frequency and ω_c is the natural cyclotron frequency of the ion.

2-Chloropyrazine, the precursor to Fe^+−2,3-didehydropyrazine, is introduced into the vacuum system through a Varian leak valve at a pressure of ca. 1.5×10^{-7} Torr. The product ion, Fe^+−2,3-didehydropyrazine, was then isolated by swept radio frequency ejection techniques[44] and allowed to react with selected neutrals introduced into the vacuum chamber by either leak valves or a solenoid pulsed valve (General Valve Corp. Series 9).[45]

All calculations were performed with the Gaussian 94 software package[46] on IBM RS 6000 RISC workstations at the Purdue University Computer Center (PUCC) and on a Silicon Graphics O2 workstation in our laboratory. The calculations were carried out by a DFT computational approach using the hybrid Becke three-parameter exchange functional, denoted here as B3LYP.[47−50] This functional was combined with the effective core potential derived by Hay and Wadt for Fe and the Dunning-Hay double-ξ basis set for C, N, and H atoms (denoted as LANL2DZ).[51] The nature of each critical point was characterized by computing the harmonic vibrational frequencies. Zero-point energy corrections were made by using a scaling factor of about 0.98. (A scaling factor of 0.989 was computed by Bauschlicher and Partridge[52] for B3LYP/6-311+G(3df,2p) and 0.980 for B3LYP/6-31G(d).)

Results and Discussion

Theory. The gas-phase geometry and thermodynamics of 2,3-didehydropyrazine (**1**) and Fe^+−2,3-didehydropyrazine (**2**) were probed by density functional theory (DFT) calculations. The optimized geometries of **1** and **2** are shown in Figure 1 with structural parameters listed in Table 1. 2,3-Didehydropyrazine has a triplet ground state with a singlet state calculated to be 9.9 kcal/mol higher in energy. Fe^+−2,3-didehydropyrazine has a sextet ground state with doublet and quartet states 4.9 and 6.8 kcal/mol higher, respectively. The bond dissociation energy for ground-state Fe^+−2,3-didehydropyrazine dissociated to Fe^+ and triplet 2,3-didehydropyrazine is calculated to be 87 ± 10 kcal/mol with zero-point energy correction. This is slightly higher than the calculated value for the related benzyne system, $D°(Fe^+-\text{benzyne}) = 76 \pm 10$ kcal/mol.[9]

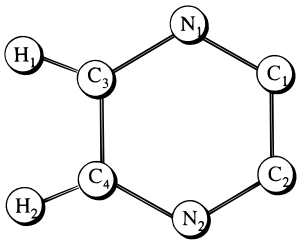

1

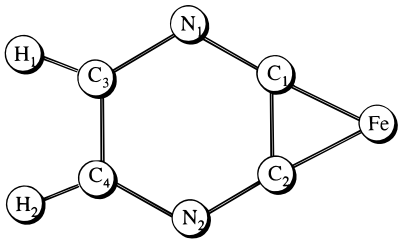

2

Figure 1. Optimized geometries of 2,3-didehydropyrazine (**1**) and Fe^+−2,3-didehydropyrazine (**2**) with parameters listed in Table 1.

Table 1. Geometries of 2,3-Dehydropyrazine (1) and Fe^+−2,3-Dehydropyrazine (2)

	2,3-didehydro-pyrazine		Fe^+−2,3-didehydro-pyrazine		
	singlet	triplet	sextet	quartet	doublet
N1−C1, Å	1.345	1.307	1.297	1.301	1.299
C1−C2, Å	1.264	1.417	1.509	1.471	1.466
C3−N1, Å	1.397	1.370	1.350	1.352	1.352
C3−C4, Å	1.420	1.408	1.426	1.430	1.430
C3−H1, Å	1.085	1.084	1.084	1.084	1.084
N1−C1−C2, deg	129.8	120.3	117.4	119.1	119.1
C3−N1−C1, deg	106.1	120.7	124.5	122.0	122.2
N1−C3−C4, deg	124.1	119.0	118.2	118.9	118.7
H1−C3−N1, deg	118.3	115.2	119.8	119.4	119.5
Fe−C1, Å			2.030	1.883	1.903
C1−Fe−C2, deg			43.7	46.0	45.3

Both the ground triplet state and the excited singlet state of 2,3-didehydropyrazine have a planar C_{2v} symmetry. The key structural differences between the triplet ground and excited singlet states involve the C1−C2 bond length and the bond angles (Table 1). The C1−C2 bond length is only 1.264 Å for the singlet state but 1.417 Å for the triplet state. In the triplet state, the ring bond angles are all nearly 120°; however, for the singlet state, the C−N−C bond angles are reduced to 106.1° and N−C1−C2 and N−C3−C4 bond angles increase to 129.8 and 124.1°, respectively. An earlier MNDO calculation predicted a large degree of biradical character in 2,3-didehydropyrazine and a remarkably long C1−C2 bond length of 1.66 Å.[29] A more recent ab initio calculation[30] yields a C1−C2 bond length of only 1.22 Å, close to our calculated value for the singlet state.

We can imagine that 2,3-didehydropyrazine is produced by the removal of two hydrogen atoms from pyrazine to yield a biradical. We now need to consider the fate of the electrons associated with the C1 and C2

(43) Gauthier, J. W.; Trautman, T. R.; Jacobson, D. B. *Anal. Chim. Acta* **1991**, *246*, 211.
(44) Comisarow, M. B.; Grassi, V.; Parisod, G. *Chem. Phys. Lett.* **1978**, *57*, 413.
(45) Carlin, T. J.; Freiser, B. S. *Anal. Chem.* **1983**, *55*, 571.
(46) Frisch, M. J.; Trucks, G. W.; Schlegel, H. B.; Gill, P. M. W.; Johnson, B. G.; Robb, M. A.; Cheeseman, J. R.; Keith, T.; Petersson, G. A.; Montgomery, J. A.; Raghavachari, K.; Al-Laham, M. A.; Zakrzewski, V. G.; Ortiz, J. V.; Foresman, J. B.; Peng, C. Y.; Ayala, P. Y.; Chen, W.; Wong, M. W.; Andres, J. L.; Replogle, E. S.; Gomperts, R.; Martin, R. L.; Fox, D. J.; Binkley, J. S.; Defrees, D. J.; Baker, J.; Stewart, J. P.; Head-Gordon, M.; Gonzalez, C.; Pople, J. A. Gaussian 94, Revision D.1; Gaussian, Inc., Pittsburgh, PA, 1995.
(47) Becke, A. D. *Phys. Rev.* **1988**, *A38*, 3098.
(48) Becke, A. D. *J. Chem. Phys.* **1993**, *98*, 1372.
(49) Becke, A. D. *J. Chem. Phys.* **1993**, *98*, 5648.
(50) Stephens, P. J.; Devlin, F. J.; Chabalowski, C. F.; Frisch, M. *J. Phys. Chem.* **1994**, *98*, 11623.
(51) Dunning, T. H., Jr.; Hay, P. J. In *Modern Theoretical Chemistry*; Schaefer, H. F., III, Ed.; Plenum: New York, 1976.
(52) Bauschlicher, C. W., Jr.; Partridge, H. *J. Chem. Phys.* **1995**, *103*, 1788.

carbon atoms. If these two electrons result in bond formation between C1 and C2, then a singlet state is produced and the C1−C2 bond distance is reduced (a C1−C2 triple bond is formed). However, if a bond is not formed, then a triplet state is produced, resulting in a longer C1−C2 bond length due to electron−electron repulsion. Hence, in our calculations, the elongation of the C1−C2 bond (1.264 Å → 1.417 Å) from the singlet to the triplet state is expected. The lone pair of electrons on the nitrogen atoms, which are in the same plane as the π-electrons of the dehydro bond, may result in a more stable polarized aromatic system. This type of polar resonance has been calculated to stabilize 2,3-didehydropyridine by an additional 0.4β.[27] Similarly, the triplet state of 2,3-didehydropyradine could also be greatly stabilized by this polarized aromatic system.

The optimized structure for the sextet ground state of Fe^+−2,3-didehydropyrazine ($^6A'$) has a slightly distorted C_{2v} symmetry. The C1−C2 bond length is elongated to 1.509 Å, compared to 1.417 Å for the triplet state of 2,3-didehydropyrazine. The metal center is coplanar with the hetaryne ring and located symmetrically with respect to the coordinated C−C bond, similar to the *o*-benzyne complexes.[3−6] The Fe−C1(2) bond length is 2.030 Å, and the C1−Fe−C2 bond angle is 43.7°.

The doublet state of Fe^+−2,3-didehydropyrazine has a similar C_{2v} structure and is less stable than the sextet state by about 4.9 kcal/mol. The C1−C2 bond length is shortened to 1.466 Å, compared to 1.509 Å in the sextet state. The Fe−C1(2) bond length also decreases to 1.903 Å in the doublet state. The quartet state of Fe^+−2,3-didehydropyrazine is 6.8 kcal/mol above the sextet ground state and again has C_{2v} symmetry. The C1−C2 bond length is 1.471 Å, and the Fe−C1(2) bond length is 1.883 Å.

The bonding for the ground state of Fe^+−2,3-didehydropyrazine can be viewed as a hetaryne π-complex or as a metallacyclopropene complex. These are the two extremes in the interaction of 2,3-didehydropyrazine with Fe^+. The C−C bond lengths in transition-metal-coordinated alkynes covers a range that spans that for free, uncoordinated alkynes (C≡C; 1.203 Å) to free, uncoordinated alkenes (C=C; 1.339 Å).[53] Cyclohexyne, unstable as a free molecule, forms a stable metal-coordinated complex with a bond length of 1.29 Å between the two coordinated carbon atoms.[54] The *o*-benzyne complex, Ta(η^5-C_5Me_5)Me_2(η^2-C_6H_4), has a C−C bond length of 1.36 Å for the two coordinated carbon atoms.[3,4] A mononuclear (η^2-*o*-benzyne)nickel(0) complex has the nickel atom coordinated by a symmetric η^2-benzyne ligand (Ni−C1 = 1.870 Å, Ni−C2 = 1.868 Å), with the coordination geometry close to trigonal planar.[6] The coordinated C−C bond length of 1.332 Å is significantly larger than those observed in alkyne complexes of zerovalent nickel and platinum.[55−57]

In contrast to transition-metal−benzyne complexes, there has not been any structural characterization for the corresponding 2,3-didehydropyrazine complexes. However, the relatively long C1−C2 bond length (1.509 Å) seems to exclude the formation of a hetaryne π-complex. A hetaryne π-complex would require that the C1−C2 bond length increase from 1.264 Å for free singlet 2,3-didehydropyrazine to 1.509 Å. However, if a metallacyclopropene-like structure is formed, then the C1−C2 bond length increases from 1.417 Å for free triplet 2,3-didehydropyrazine to 1.509 Å. This is still a large increase in C1−C2 bond length upon coordination but much smaller than that for the hetaryne π-complex. Consequently, we favor a metallacyclopropene-like bonding structure for the Fe^+−2,3-didehydropyrazine complex.

Experimental Results. **2-Chloropyrazine**. Fe^+ reacts with 2-chloropyrazine to yield exclusive HCl loss (reaction 1; $k = 4.5 \times 10^{-10}$ cm^3 molecule^{-1} s^{-1}, efficiency 27%). $FeC_4N_2H_2^+$, formed in reaction 1, is unreactive

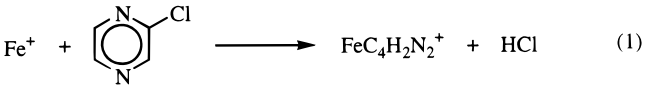

(1)

with 2-chloropyrazine. CID of $FeC_4N_2H_2^+$ yields exclusive formation of Fe^+. $FeC_4H_2N_2^+$ is believed to consist of 2,3-didehydropyrazine bound to Fe^+ (structure **2**). The CID results suggest that 2,3-didehydropyrazine has an IP less than that of Fe (IP = 7.87 eV).[58]

Ethene and Ethene-*d*$_4$. $FeC_4H_2N_2^+$ (**2**) reacts slowly with ethene and ethene-d_4 to yield exclusive formation of the adducts $FeC_4H_2N_2C_2H_4^+$ and $FeC_4H_2N_2C_2D_4^+$ (reactions 2 and 3; $k = 7.5 \times 10^{-12}$ cm^3 molecule^{-1} s^{-1}, efficiency 0.80%). CID on $FeC_4H_2N_2C_2H_4^+$, generated

$$FeC_4H_2N_2^+ + C_2H_4 \rightarrow FeC_4H_2N_2C_2H_4^+ \quad (2)$$

$$FeC_4H_2N_2^+ + C_2D_4 \rightarrow FeC_4H_2N_2C_2D_4^+ \quad (3)$$

from C_2H_4, and on $FeC_4H_2N_2C_2D_4^+$, generated from C_2D_4, yield only $FeC_4H_2N_2^+$ (C_2H_4/C_2D_4 loss) and Fe^+ over the energy range studied (1−30 eV). To further probe the structure of these ethene adducts, the product ions were isolated and reacted with toluene. Each of the products produced in reactions 2 and 3 gives exclusive ethene displacement to yield $FeC_4H_2N_2C_7H_8^+$ (i.e., no isotopic exchange is observed for the deuterated species). These results suggest that a simple ethene adduct is formed (i.e., no C−C bond formation with ethene has occurred). In contrast, Fe(*o*-benzyne)$^+$ reacts with ethene to yield Fe^+, $FeC_6H_6^+$ (C_2H_2 loss), $FeC_8H_6^+$ (H_2 loss), and $FeC_8H_8^+$ (adduct formation).[11]

Ethyne and Ethyne-*d*$_2$. Reaction of **2** with C_2H_2 and C_2D_2 yields adducts exclusively (reactions 4 and 5: $k = 5.8 \times 10^{-11}$ cm^3 molecule^{-1} s^{-1}, efficiency 6.3%). This is

$$FeC_4H_2N_2^+ + C_2H_2 \rightarrow FeC_6H_2N_2^+ \quad (4)$$

$$FeC_4H_2N_2^+ + C_2D_2 \rightarrow FeC_6H_2D_2N_2^+ \quad (5)$$

surprisingly fast kinetics for adduct formation and roughly 1 order of magnitude faster than the ethene reaction. These adducts were probed to determine if the

(53) Lide, D. R. *CRC Handbook of Chemistry and Physics*, 79th ed.; CRC Press: Boca Raton, FL, 1998.
(54) Whimp, P. O. *J. Organomet. Chem.* **1971**, *32*, C69.
(55) Ittel, S. D.; Ibers, J. A. *Adv. Organomet. Chem.* **1976**, *14*, 33.
(56) Dickson, R. S.; Ibers, J. A. *J. Organomet. Chem.* **1972**, *36*, 191.
(57) Robertson, G. B.; Whimp, P. O. *J. Am. Chem. Soc.* **1975**, *97*, 1051.
(58) Lias, S. G.; Bartmess, J. E.; Liebman, J. F.; Holmes, J. L.; Levin, R. D.; Mallard, W. G. Gas-Phase Ion and Neutral Thermochemistry. *J. Phys. Chem. Ref. Data* **1988**, *17*, Suppl. No. 1.

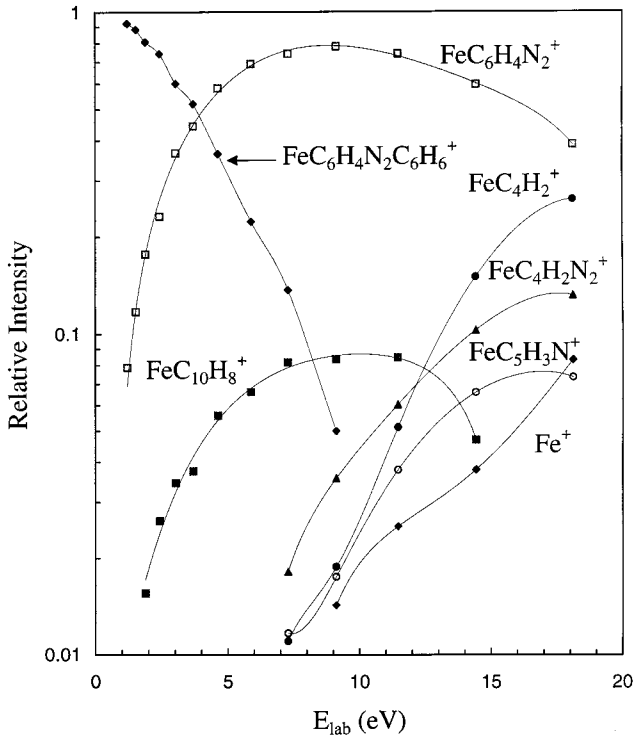

Figure 2. Energy-resolved CID breakdown curve of $FeC_6H_4N_2C_6H_6^+$, produced by reaction of benzene with $FeC_6H_4N_2^+$ formed in reaction 2.

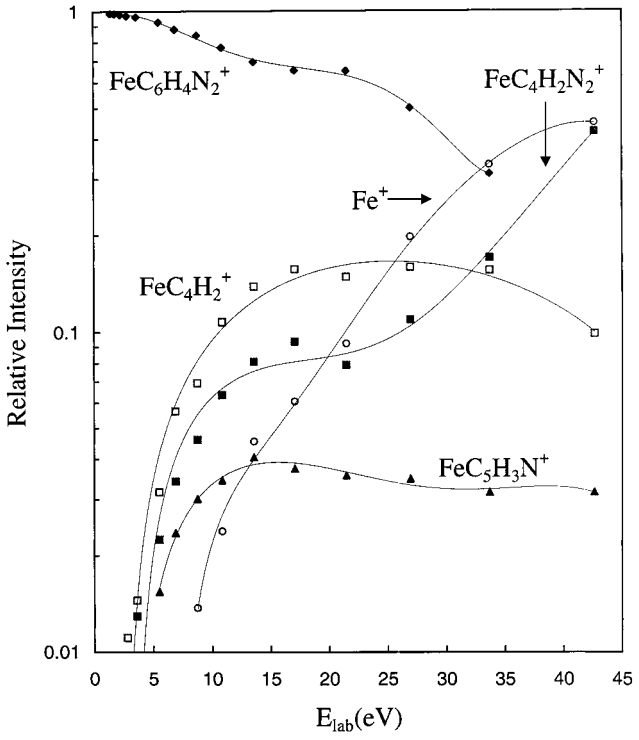

Figure 3. Energy-resolved CID breakdown curve of $FeC_6H_4N_2^+$ formed by reaction 2.

ethyne unit has undergone coupling to the 2,3-didehydropyrazine ligand by reaction with benzene and CID. In contrast to the ethene adducts produced in reactions 2 and 3, reactions of these ethyne adducts with benzene only yield benzene adducts (i.e., no C_2H_2/C_2D_2 displacement is observed). The CID breakdown curve for the benzene adduct yields initial benzene elimination (Figure 2). At higher energy, additional fragmentations are observed (vide infra). The absence of ethyne displacement, in both the reaction with benzene and CID of the benzene adduct, suggests that ethyne is incorporated into the $C_4H_2N_2$ ligand ($D°(Fe^+-C_2H_2) = 32 \pm 6$ kcal/mol;[59] $D°(Fe^+-C_6H_6) = 49.6 \pm 2.3$ kcal/mol[60]). In addition, CID of the ethyne adducts produced in reactions 4 and 5 yield several products. For example, CID of the $FeC_6H_4N_2^+$ adduct yields $FeC_4H_2N_2^+$ (C_2H_2 loss), $FeC_5H_3N^+$ (HCN loss), $FeC_4H_2^+$ ($C_2H_2N_2$ loss), and Fe^+ (Figure 3; reactions 6−9). These results indicate that

$$FeC_6H_4N_2^+ \xrightarrow{CID} \begin{cases} FeC_4H_2N_2^+ + C_2H_2 & (6) \\ FeC_5H_3N^+ + HCN & (7) \\ FeC_4H_2^+ + 2\,HCN & (8) \\ Fe^+ + (C_6H_4N_2) & (9) \end{cases}$$

ethyne has coupled to the 2,3-didehydropyrazine ligand. Process 8 presumably involves the elimination of two HCN molecules instead of an intact $C_2H_2N_2$ unit. Formation of $FeC_4H_2^+$ is competitive with direct C_2H_2 loss at low energies. At higher energy, $FeC_4H_2N_2^+$ (C_2H_2 loss) and Fe^+ dominate. As with CID, formation of $FeC_4H_2^+$ (loss of 2 HCN) and $FeC_4H_2N_2^+$ (C_2H_2 loss) are competitive processes at low energies for SORI-CID (Figure 4). Interestingly, loss of two HCN molecules is dominant over loss of one HCN molecule at low energy for both CID and SORI-CID.

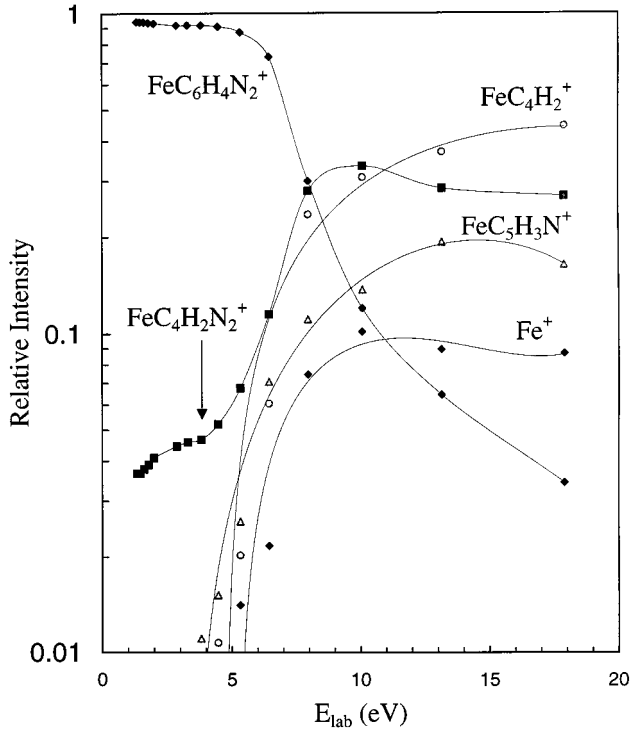

Figure 4. Energy-resolved SORI-CID breakdown curve of $FeC_6H_4N_2^+$ formed by reaction 2.

The CID and SORI-CID breakdown curves for $FeC_6H_2D_2N_2^+$, produced in reaction 5 from C_2D_2, are il-

(59) MacMahon, T. J.; Jackson, T. C.; Freiser, B. S. *J. Am. Chem. Soc.* **1989**, *111*, 421.
(60) Meyer, F.; Khan, F. A.; Armentrout, P. B. *J. Am. Chem. Soc.* **1995**, *117*, 9740.

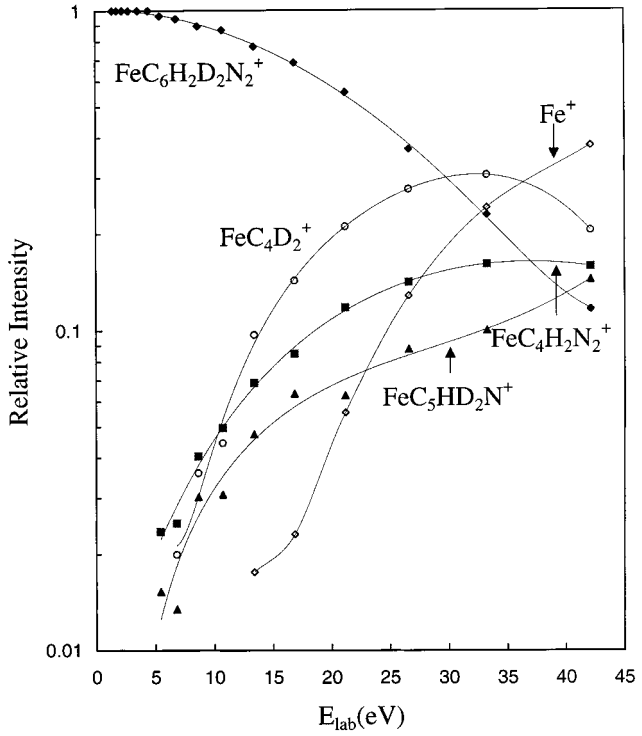

Figure 5. Energy-resolved CID breakdown curve of $FeC_6H_2D_2N_2^+$ formed by reaction 3.

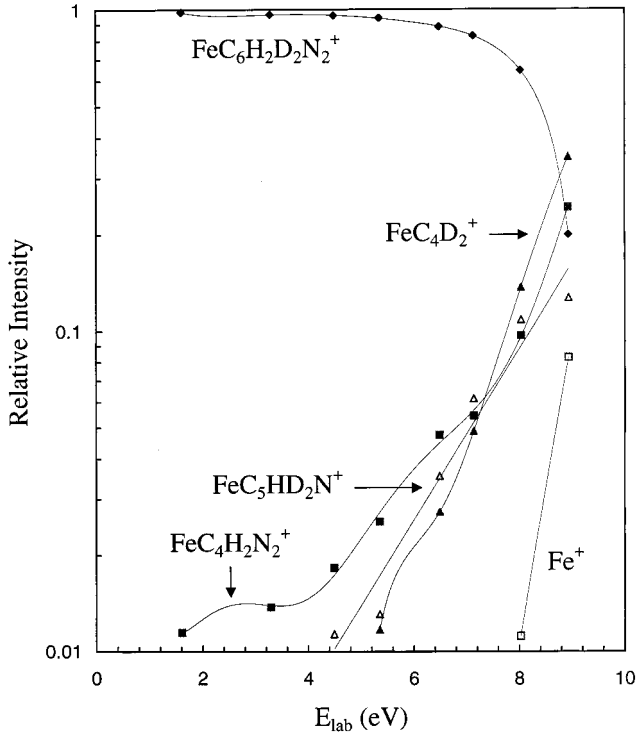

Figure 6. Energy-resolved SORI-CID breakdown curve of $FeC_6H_2D_2N_2^+$ formed by reaction 3.

lustrated in Figures 5 and 6, respectively. The decompositions are summarized in reactions 10−13. It is noteworthy that ethyne loss occurs *exclusively* as C_2D_2 and hydrogen cyanide losses occur exclusively as HCN. Consequently, there is *no* isotopic scrambling in the decomposition of the C_2D_2 adduct, despite obvious ligand coupling.

Ligand coupling presumably involves the addition of ethyne across the hetaryne triple bond to yield initially

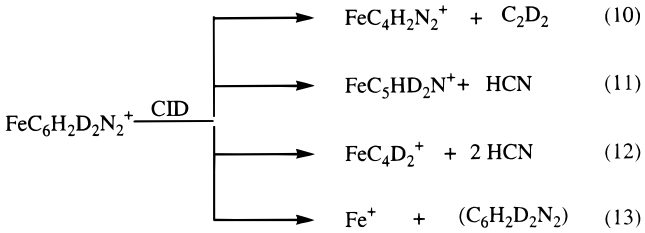

3 (Scheme 1). **3** could then collapse to **5** or undergo hydrogen migration to yield **6**. The initial step in the reaction could also involve insertion into the acetylenic C−H bond to yield **4**, which subsequently rearranges to **6** (Scheme 1). Fe(*o*-benzyne)$^+$ reacts with C_2H_2 to yield exclusive formation of Fe^+ (reaction 14).[17] The

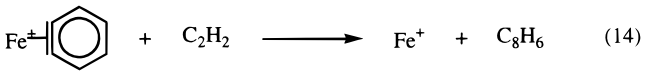

structure of the neutral C_8H_6 could be either **7** or **8**. Formation of **7** would be 40 kcal/mol *endothermic*, whereas formation of **8** would be 6 kcal/mol *exothermic* for reaction 14.[61] Therefore, C_8H_6 formation in reaction 14 is most likely structure **8**.

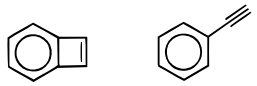

7 **8**

The formation of **8** in reaction 14 supports the generation of **6** in reactions 4 and 5. As **8** is 46 kcal/mol more stable than **7**, **6** may be equal more stable than **5**. Hence, we will consider the fragmentation of the $FeC_6H_4N_2^+$ product as originating from **6**. C_2H_2 loss may proceed by the reverse of Scheme 1. This mechanism predicts loss of ethyne as C_2D_2 for CID of the $FeC_6H_2D_2N_2^+$ adduct formed in reaction 5 (i.e., no isotopic scrambling). The HCN losses result in cleavage of the six-membered ring, leaving behind a C_4H_2 unit. This ligand is most likely 1,3-butadiyne. The loss of HCN can proceed by the electron shifts depicted in Scheme 2 which yield three ligands bond to Fe^+. The activated species then eliminates HCN, which is more weakly bound to Fe^+ than alkynes. Again, Scheme 2 predicts loss of HCN from the $FeC_6H_2D_2N_2^+$ adduct formed in reaction 5.

The SORI-CID results (Figure 4) indicate that the two decomposition channels, C_2H_2 loss (reaction 6) and loss of two HCN molecules (reaction 8), are competitive processes. This suggests that they have similar energy requirements (barriers). For CID (Figure 3), loss of two HCN molecules dominates at low energy, with C_2H_2 loss dominating at high energy. The rearrangement resulting in loss of two HCN molecules (Scheme 2) is apparently more kinetically constrained than that for C_2H_2 elimination (Scheme 1). The fact that loss of two HCN molecules dominates over loss of one HCN molecule suggests a significant barrier for the rearrangement depicted in Scheme 2. Consequently, intermediate **9** is formed with internal energy in excess of that required for the elimination of two HCN molecules.

Propene and Isobutene. In contrast to ethene and ethyne, both propene and isobutene do not yield adducts

(61) This calculation is based on heats of formation taken from ref 57.

Scheme 1

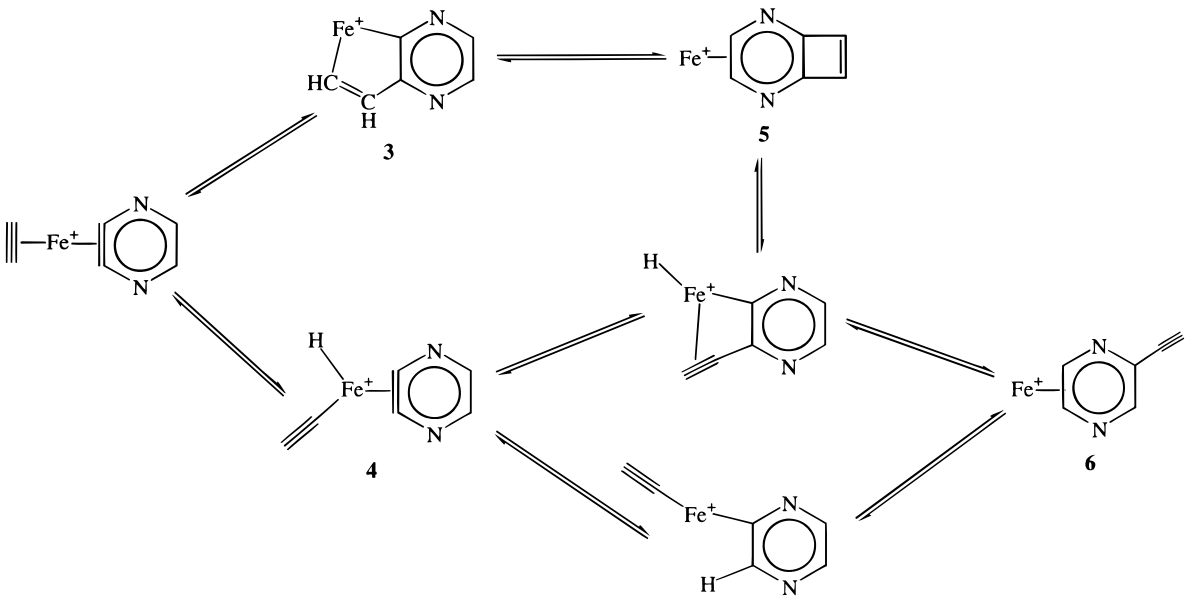

Scheme 2

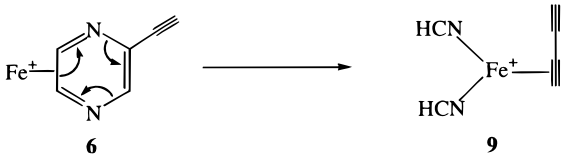

with $FeC_4H_2N_2^+$. Instead, they react at moderate rates ($k = 1.5 \times 10^{-10}$ cm^3 molecule^{-1} s^{-1}, efficiency 14% for propene; $k = 1.8 \times 10^{-10}$ cm^3 molecule^{-1} s^{-1}, efficiency 16% for isobutene) to yield simple neutral losses (reactions 15−18). Surprisingly, both reactants yield the same products.

$$FeC_4H_2N_2^+ + \text{propene} \xrightarrow{70\%} FeC_7H_6N_2^+ + H_2 \quad (15)$$

$$\xrightarrow{30\%} FeC_5H_6N_2^+ + C_2H_2 \quad (16)$$

$$FeC_4H_2N_2^+ + \text{isobutene} \xrightarrow{90\%} FeC_7H_6N_2^+ + CH_4 \quad (17)$$

$$\xrightarrow{10\%} FeC_5H_6N_2^+ + C_3H_4 \quad (18)$$

CID of $FeC_5H_6N_2^+$, formed in reactions 16 and 18, yields exclusive Fe^+ formation ($C_5H_6N_2$ loss; reaction 19). CID of $FeC_7H_6N_2^+$, formed in reactions 15 and 17, yields both Fe^+ and $C_7H_6N_2^+$ (reactions 20 and 21), with $C_7H_6N_2^+$ dominating at all energies (Figures 7 and 8).

$$FeC_5H_6N_2^+ \xrightarrow{CID} Fe^+ + C_5H_6N_2 \quad (19)$$

$$FeC_7H_6N_2^+ \xrightarrow{CID} Fe^+ + C_7H_6N_2 \quad (20)$$

$$\longrightarrow C_7H_6N_2^+ + Fe \quad (21)$$

These CID results clearly indicate that the olefins have coupled to the 2,3-didehydropyrazine ligand in reactions 15−18. $FeC_5H_6N_2^+$ simply consists of CH_4 added to the $C_4H_2N_2$ ligand (a methanation process), presumably added across the heteryne bond to yield Fe^+−methylpyrazine. The CID results are consistent with formation of Fe^+−methylpyrazine in reactions 16 and 18, since the IP of methylpyrazine should be greater than that of Fe (IP(Fe) = 7.87 eV, IP(pyrazine) = 9.29 eV).[58] The structure of $FeC_7H_6N_2^+$, produced in reactions 15 and 17, however, is open to more speculation. What is clear is that it consists of a single ligand and that the IP of the $C_7H_6N_2$ ligand is close to or slightly lower than that for Fe.

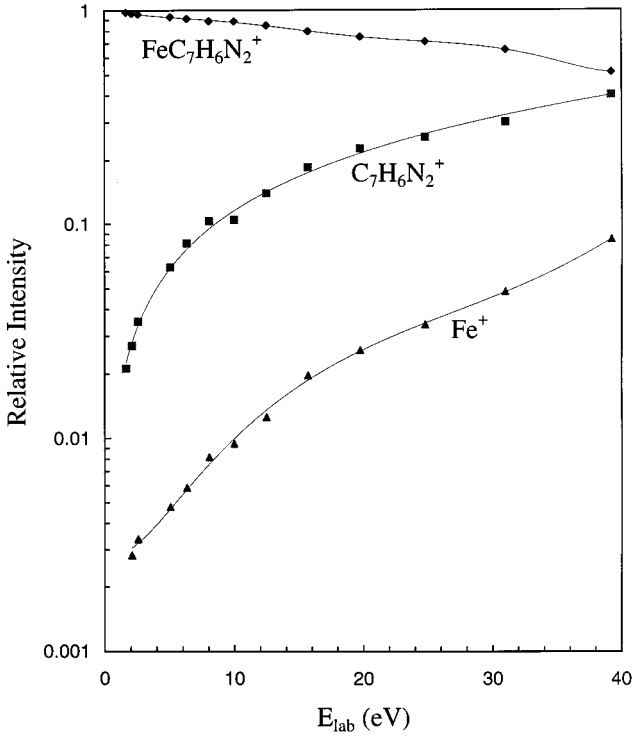

Figure 7. Energy-resolved CID breakdown curve of $FeC_7H_6N_2^+$ formed by reaction 15.

We now consider mechanisms for formation of the products in reactions 15−18. Initially, the collision complex **10** may undergo activation of the allylic carbon−hydrogen bond to form **11** (Scheme 3). The reversible insertion into allylic carbon−hydrogen bonds has frequently been invoked in mechanisms for catalytic isomerization of olefins by transition-metal complexes.[62]

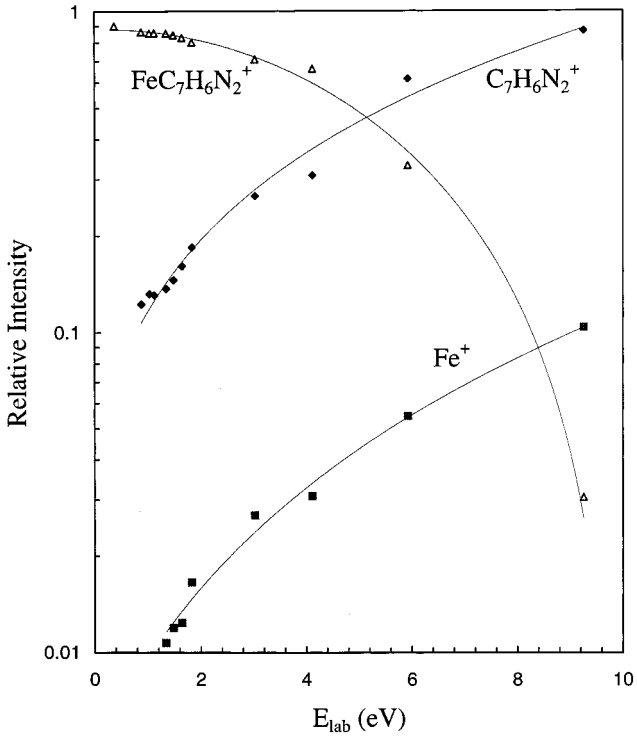

Figure 8. Energy-resolved SORI-CID breakdown curve of $FeC_7H_6N_2^+$ formed by reaction 15.

In addition, this process is often observed in gas-phase transition-metal-ion chemistry.[63] The hydrido−allyl intermediate **11** then undergoes migratory insertion of either the allyl group or the hydride into the 2,3-didehydropyrazine triple bond to form **12** and **13**, respectively. **12** can undergo hydride insertion to produce either **14** or **15**. **14**, a metallacyclohexane, can undergo reductive elimination to produce **16** followed by dehydrogenation (propene) or demethanation (isobutene) to yield **17** (the pyrazine analogue of indene). Intermediate **13** can undergo allyl migratory insertion to also yield **15**. **15** can undergo hydrogen migration to yield **18** followed by elimination of an alkyne to yield **19**.

The proposed mechanism outlined in Scheme 3 demands that the terminal carbon atoms of propene appear in equal amounts in the methanation product, **19**. Consequently, $FeC_4H_2N_2^+$ was reacted with [1-^{13}C]-propene. The methanation product consists of 51% $FeC_4{}^{13}CH_6N_2^+$ and 49% $FeC_5H_6N_2^+$, as demanded by this mechanism. The reactions with propene and isobutene are ca. 15% efficient. We believe that the bottleneck in these reactions is the initial activation of the allylic carbon−hydrogen bond to yield **11**. One troubling aspect of the mechanism outlined in Scheme 3 is the complete absence of dehydrogenation for reaction with isobutene. We expect that intermediate **16** could yield both demethanation and dehydrogenation with isobutene.

Other mechanisms have been proposed to account for the reactions of olefins with metal ion−(*o*-benzyne) complexes that involve either direct coupling of the ligands (ene mechanism) or direct insertion of the metal ion into a vinylic bond of the olefin.[11] We feel that these mechanisms are not operative here due to the inert behavior of ethene combined with the isotopic results for [1-^{13}C]propene.

Propyne and Allene. The C_3H_4 isomers propyne and allene yield the same products with similar distributions upon reaction with $FeC_4H_2N_2^+$ (reactions 22−27). These

$FeC_6H_2N_2^+ + C_3H_4$	propyne	allene	
→ $FeC_7H_6N_2^+$	5%	3%	(22)
→ $FeC_7H_4N_2^+ + H_2$	4%	2%	(23)
→ $FeC_5H_4N_2^+ + C_2H_2$	6%	9%	(24)
→ $FeC_6H_5N^+ + HCN$	22%	16%	(25)
→ $Fe^+ + C_7H_6N_2$	57%	61%	(26)
→ $C_7H_6N_2^+ + Fe$	6%	9%	(27)

reactions seem to share features in common with those for both ethyne and propene reactions. For example, reactions 26 and 27 are analogous to reaction 15 with subsequent CID for propene. The $C_7H_6N_2$ product again is presumably the pyrazine analogue of indene. Reactions 24 and 25 are analogous to the CID processes for the ethyne adduct, $FeC_6H_4N_2^+$, formed in reaction 4.

A mechanism for reaction of propyne and allene with $FeC_4H_2N_2^+$ is presented in Scheme 4. The initial steps in Scheme 4 are analogous to those for ethyne. Ultimately, species **20** and **21** can be formed. **21** subsequently decomposes to yield both Fe^+ and $C_7H_6N_2^+$ due to their similar IP's (vide supra).

The loss of HCN (reaction 25) may involve the decomposition of **20**. As with **6**, **20** can undergo rearrangement by electron shifts, as depicted in Scheme 5, to yield the bis-HCN complex **23**, which eliminates an HCN molecule. However, CID of $FeC_6H_5N^+$, produced in reaction 25, yields predominant C_6H_5N loss with only a small amount of HCN loss (Figure 9; reactions 28 and 29). These CID results suggest that $FeC_6H_5N^+$ consists

$FeC_6H_5N^+$	$\xrightarrow{CID}$ $Fe^+ + C_6H_5N$		(28)
	→ $FeC_5H_4^+ + HCN$		(29)

of an intact C_6H_5N ligand rather than two ligands (HCN and C_5H_4) as predicted in Scheme 5. In contrast to the CID breakdown curve (Figure 9), the SORI-CID breakdown curve yields both Fe^+ and $FeC_5H_4^+$ in significant amounts (Figure 10). This suggests that there are similar energy requirements (barriers) for both reactions 28 and 29. The low amount of reaction 29 in the CID breakdown curve is simply due to kinetic constraints involved in rearrangement leading to HCN extrusion.

We now consider how the $FeC_7H_6N_2^+$ intermediate eliminates HCN. As with **6**, intermediate **20** would be expected to rearrange to **23** (Scheme 5). The CID results for $FeC_6H_5N^+$, formed in reaction 25, clearly suggest that such a rearrangement has not occurred. Intermediate **21** would simply undergo simple ligand loss, produc-

(62) Webb, G. In *Catalysis*; Specialists Periodical Report 2; Kemball, C., Dowden, D. A., Eds.; The Chemical Society: London, 1977; pp 151−163.

(63) Byrd, G. D.; Freiser, B. S. *J. Am. Chem. Soc.* **1982**, *104*, 5944.

Scheme 3

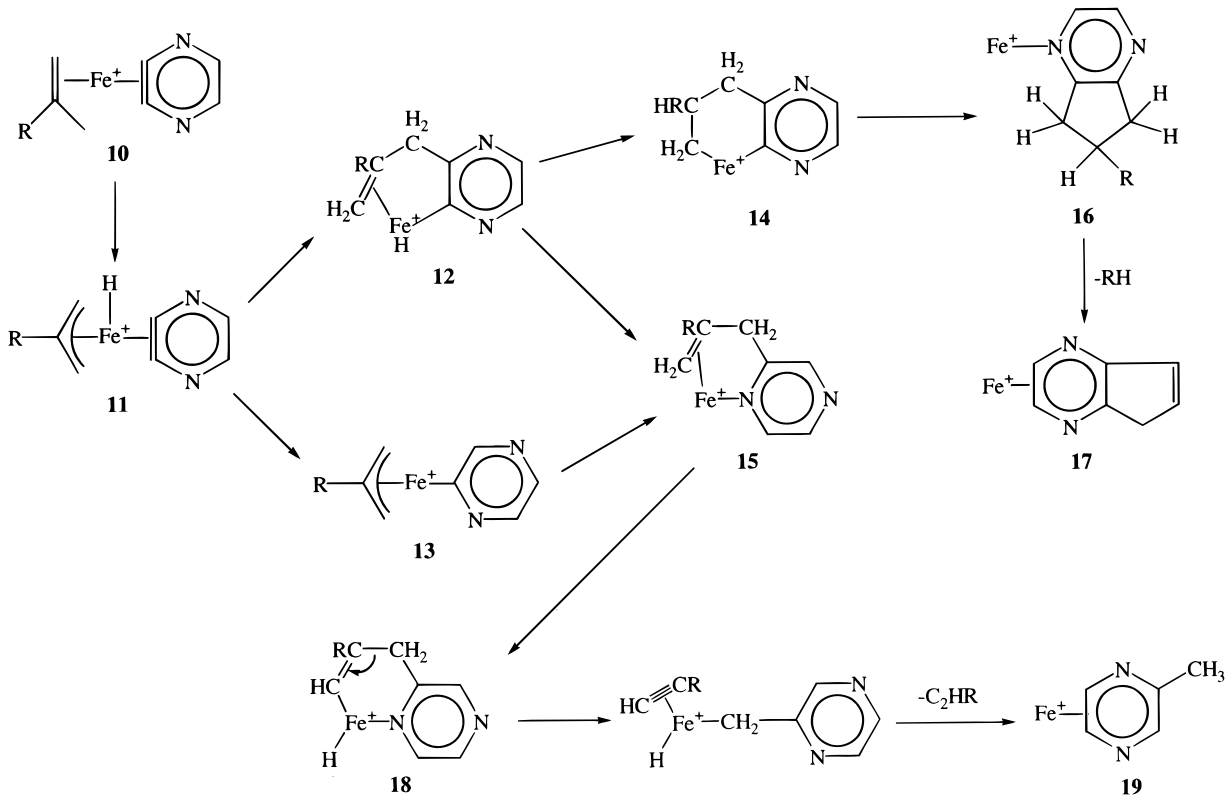

Scheme 4

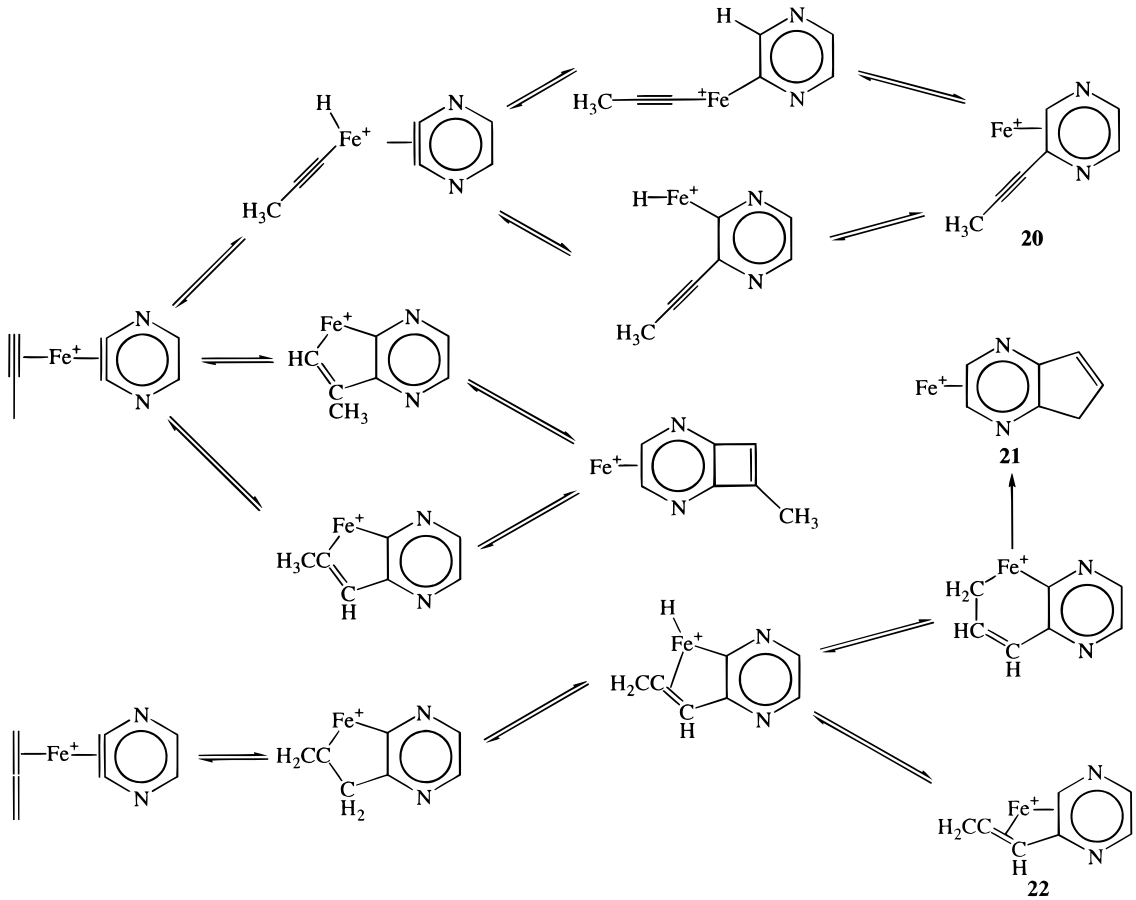

ing Fe^+ or $C_7H_6N_2^+$. Intermediate **22**, however, may undergo ring expansion to yield a seven-membered ring (Scheme 6; **24**). **24** may then extrude HCN to yield the five-membered-ring compounds **25** and **26**. These five-membered-ring species then either undergo complete loss of the ligand or rearrangement, yielding HCN

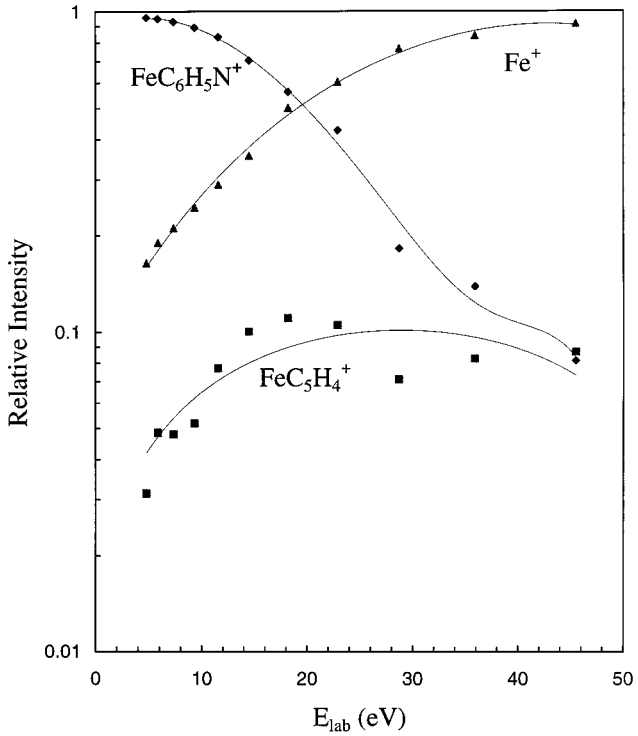

Figure 9. Energy-resolved CID breakdown curve of $FeC_6H_5N^+$ formed by reaction 25.

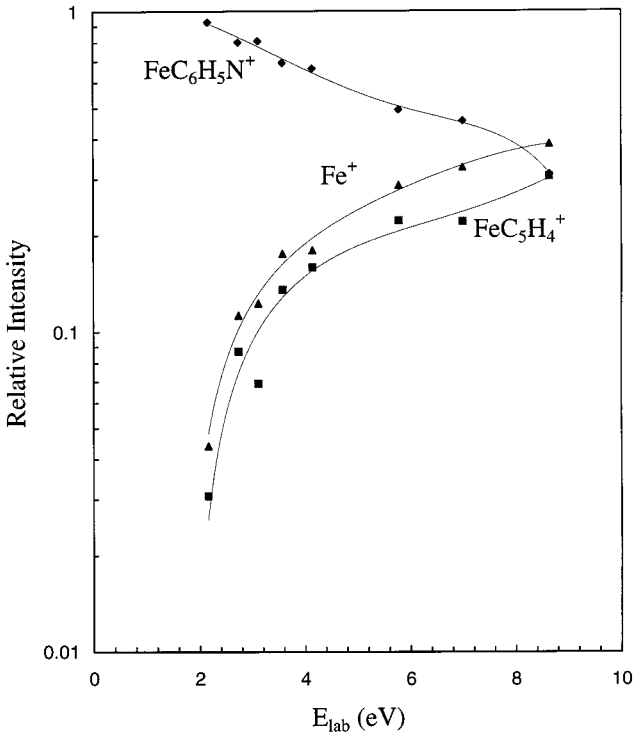

Figure 10. Energy-resolved SORI-CID breakdown curve of $FeC_6H_5N^+$ formed by reaction 25.

Scheme 5

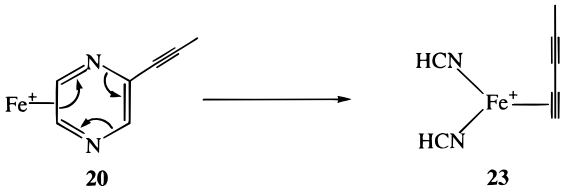

elimination upon activation. Such a ring expansion is not available to intermediate **6**.

1-Butene, *cis*-2-Butene, and 1,3-Butadiene. The reactions of 1-butene and *cis*-2-butene with $FeC_4H_2N_2^+$ are complex, as evidenced by the many products (reactions 30−36). As expected, both butenes yield the same

$FeC_4H_2N_2^+ + C_4H_8$

		1-butene	*cis*-2-butene	
→	$FeC_8H_{10}N_2^+$	7%	5%	(30)
→	$FeC_4H_4N_2^+ + C_4H_6$	5%	6%	(31)
→	$FeC_5H_6N_2^+ + C_3H_4$	1%	1%	(32)
→	$FeC_6H_6N_2^+ + C_2H_4$	10%	12%	(33)
→	$FeC_6H_8N_2^+ + C_2H_2$	2%	4%	(34)
→	$FeC_8H_6N_2^+ + 2H_2$	39%	35%	(35)
→	$FeC_8H_8N_2^+ + H_2$	36%	37%	(36)

products with similar product distributions. In contrast, Fe(*o*-benzyne)$^+$ reacts with both butenes to give mainly the product ions from methanation (reaction 32) and

Scheme 6

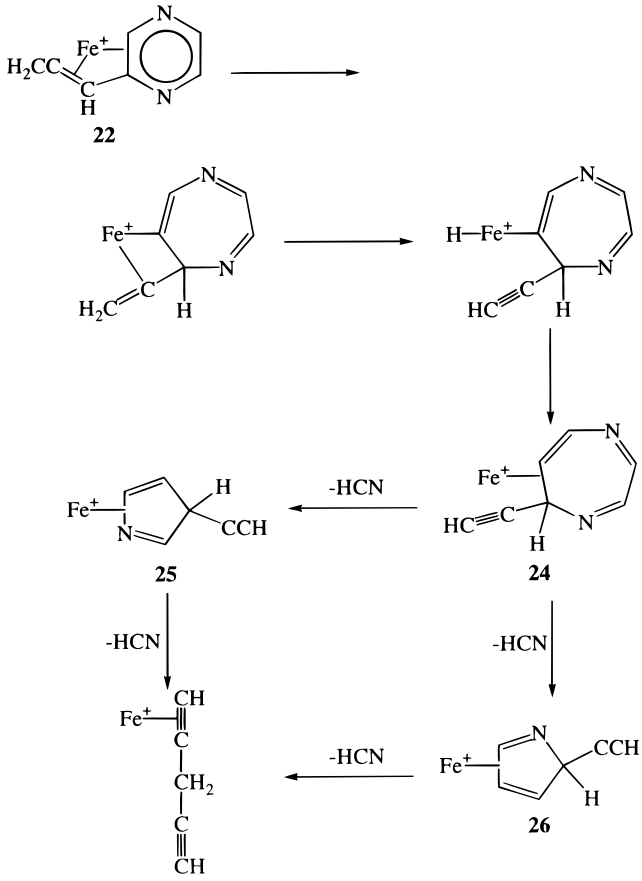

dehydrogenation (reactions 35 and 36).[11] However, only 1% methanation product was observed in the case of Fe^+−2,3-didehydropyrazine, while dehydrogenation dominates in both systems. 1,3-Butadiene reacts with $FeC_4H_2N_2^+$ to yield exclusive dehydrogenation (reaction

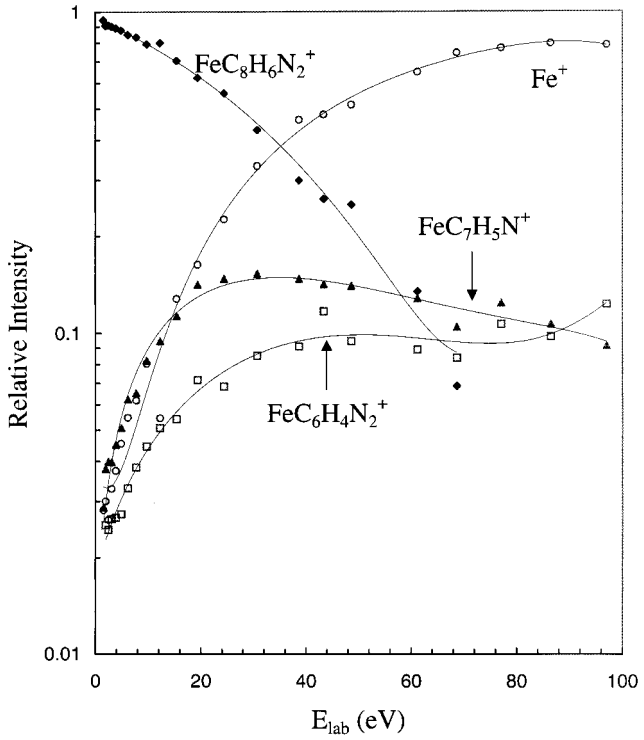

Figure 11. Energy-resolved CID breakdown curve of $FeC_8H_6N_2^+$ formed by reaction 35.

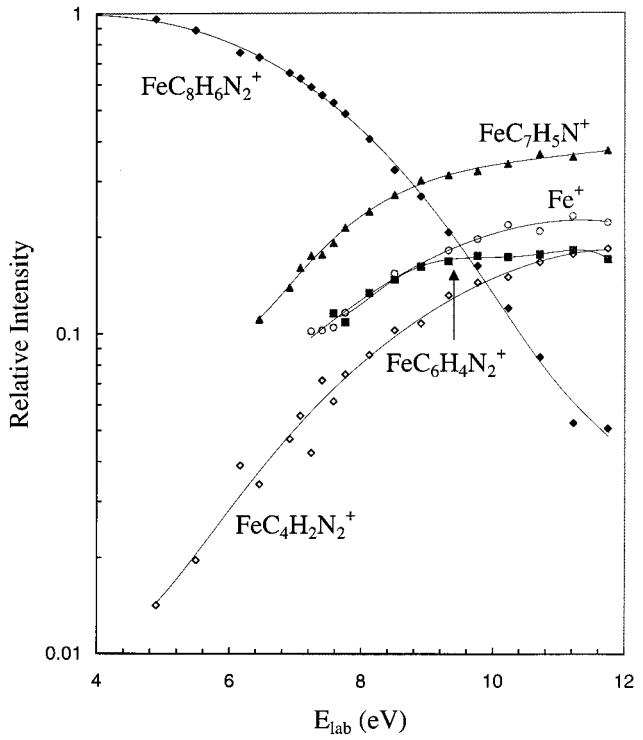

Figure 12. Energy-resolved SORI-CID breakdown curve of $FeC_8H_6N_2^+$ formed by reaction 35.

Scheme 7

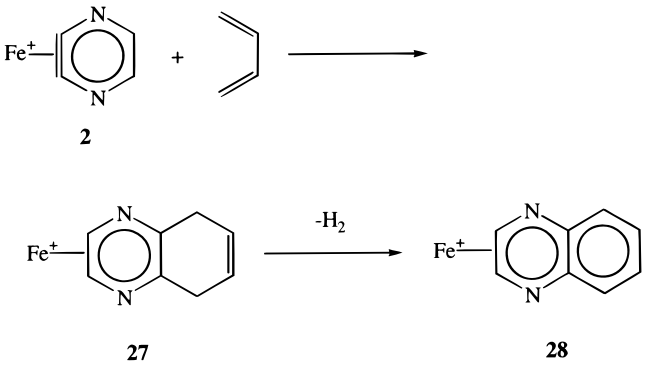

37). Due to the complexity of the linear butene reactions

$$FeC_4H_2N_2^+ + C_4H_6 \rightarrow FeC_8H_6N_2^+ + H_2 \quad (37)$$

we will not consider reaction mechanisms. However, the 1,3-butadiene reaction is much simpler with only one product observed.

Reaction 37 may simply involve the addition of 1,3-butadiene across the hetaryne bond to yield **27** followed by dehydrogenation to yield an Fe(quinoxaline)$^+$ complex, **28** (Scheme 7). Reaction of 1,3-butadiene-d_6 yields exclusive D_2 loss, as predicted for Scheme 7. CID of the $FeC_8H_6N_2^+$ ion formed in reaction 37 yields exclusive Fe^+ formation. CID of an authentic Fe(quinoxaline)$^+$ complex yields an identical CID breakdown curve, with Fe^+ the only fragment ion. In contrast, the CID breakdown curve for $FeC_8H_6N_2^+$, produced in reaction 35 (1-butene), yields additional fragmentations (Figure 11; reactions 38−40), with Fe^+ the dominant channel. SORI-CID of this same $FeC_8H_6N_2^+$ ion yields four predominant fragmentations (Figure 12) with $FeC_4H_2N_2^+$ formation (C_4H_4 loss) also observed. These results

$$FeC_8H_6N_2^+ \xrightarrow{\text{CID}} \begin{cases} FeC_6H_4N_2^+ + C_2H_2 & (38) \\ FeC_7H_5N^+ + HCN & (39) \\ Fe^+ + (C_8H_6N_2) & (40) \end{cases}$$

suggest that this $FeC_8H_6N_2^+$ consists of an entirely different structure than Fe(quinoxaline)$^+$ or a mixture of structures.

The bond dissociation energy (BDE) of Fe^+−quinoxaline was estimated by using ion−molecule reactions with benzene, ammonia, and propene. Reactions of Fe(quinoxaline)$^+$ with ammonia and propene yield only adduct formation, and CID on the adducts gives Fe(quinoxaline)$^+$ exclusively, suggesting that $D°(Fe^+-\text{quinoxaline}) > D°(Fe^+-NH_3) = 42.8$ kcal/mol,[64] $D°(Fe^+-\text{quinoxaline}) > D°(Fe^+-C_3H_6) = 37 \pm 2$ kcal/mol.[65] Reaction of Fe(quinoxaline)$^+$ with benzene yields Fe(benzene)$^+$ and the adduct Fe(quinoxaline)(benzene)$^+$. CID of this adduct yields predominantly $FeC_6H_6^+$ with only a minor amount of Fe(quinoxaline)$^+$ observed. These ligand displacement reactions combined with the CID results suggest that $D°(Fe^+-\text{quinoxaline})$ is only slightly less than $D°(Fe^+-C_6H_6) = 49.6 \pm 2.3$ kcal/mol.[60] From these results we assign $D°(Fe^+-\text{quinoxaline}) = 47 \pm 5$ kcal/mol.

Summary

Fe^+−2,3-didehydropyrazine (**2**) is generated by reaction of Fe^+ with chloropyrazine, resulting in HCl elimination. **2** is unreactive with chloropyrazine, and CID of **2** yields exclusive formation of Fe^+ (i.e., $C_4H_2N_2$ loss).

(64) Langhoff, S. R.; Bauschlicher, C. W.; Partridge, H.; Sodupe, M. *J. Chem. Phys.* **1991**, *95*, 10677.
(65) Jacobson, D. B.; Freiser, B. S. *J. Am. Chem. Soc.* **1983**, *105*, 7484.

In contrast to the *o*-benzyne system, our calculations found that the ground state of 2,3-didehydropyrazine is the triplet state, which lies 9.9 kcal/mol below the singlet state. The interaction between the two dehydro bonds with the electron lone pairs on the adjacent nitrogen atoms would result in a polar resonance form which apparently stabilizes the triplet state. Both the ground state (sextet) and the excited states (doublet and quartet) of Fe^+−2,3-didehydropyrazine have slightly distorted C_{2v} symmetries in which the metal center is coplanar with the 2,3-didehydropyrazine ring and is inserted symmetrically into the C−C triple bond, forming a pyrazinometallacyclopropene complex. The computed bond dissociation energy for the sextet $D°(Fe^+-$2,3-didehydropyrazine) is 87 ± 10 kcal/mol, which is slightly higher than that found for Fe^+−*o*-benzyne (76 ± 10 kcal/mol).[9]

The reactivity of Fe^+−*o*-benzyne and Fe^+−2,3-didehydropyrazine (**2**) with simple olefins and alkynes are quite variable; whereas Fe^+−*o*-benzyne undergoes a ligand coupling reaction with ethene, **2** only forms a simple adduct. Both arynes, however, react with ethyne by ligand coupling. Overall, **2** has a richer and more complex reactivity than Fe^+−*o*-benzyne with three- and four-carbon unsaturated hydrocarbons. For example, reactions of **2** with propyne, allene, 1-butene, and *cis*-2-butene yield numerous products. In contrast, **2** reacts with 1,3-butadiene to yield a simple product ($FeC_8H_6N_2^+$) by dehydrogenation. The CID breakdown curve of this product ion is identical with that for authentic Fe^+-quinoxaline. Ligand displacement reactions yield a bond dissociation energy of 47 ± 5 kcal/mol for $D°(Fe^+-$quinoxaline). Propene and isobutene react with **2** to yield $FeC_5H_6N_2^+$ and $FeC_7H_6N_2^+$, presumably via a metal-centered mechanism. It is proposed that these reactions occur initially by activation of the allylic C−H bond followed by migratory insertion of either the allyl group or the hydride into the 2,3-didehydropyrazine triple bond. $FeC_5H_6N_2^+$ is presumed to be Fe^+−methylpyrazine, and the intact ligand of $FeC_7H_6N_2^+$ is likely the pyrazine analogue of indene. Apparently, two mechanisms proposed for the Fe^+−*o*-benzyne system are not operating here.

Acknowledgment is made to the Division of Chemical Sciences in the Office of Basic Energy Sciences of the United States Department of Energy (under Grant No. DE-FG02-87ER13766) for supporting this research.

OM980924J